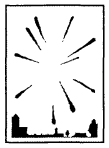

Meteoritics & Planetary Science 36, 1605–1616 (2001)
Available online at http://www.uark.edu/meteor

The NEAR–Shoemaker x-ray/gamma-ray spectrometer experiment: Overview and lessons learned

J. I. TROMBKA[1]*, L. R. NITTLER[2], R. D. STARR[3], L. G. EVANS[4], T. J. McCOY[5], W. V. BOYNTON[6], T. H. BURBINE[5], J. BRÜCKNER[7], P. GORENSTEIN[8], S. W. SQUYRES[9], R. C. REEDY[10], J. O. GOLDSTEN[11], L. LIM[9], K. HURLEY[12], P. E. CLARK[3], S. R. FLOYD[1], T. P. McCLANAHAN[1], E. McCARTNEY[9], J. BRANSCOMB[9], J. S. BHANGOO[5], I. MIKHEEVA[5] AND M. E. MURPHY[1]

[1]Goddard Space Flight Center, Laboratory for Extraterrestrial Physics, Code 691, Greenbelt, Maryland 20771, USA
[2]Carnegie Institution of Washington, Department of Terrestrial Magnetism, 5241 Broad Branch Road Northwest, Washington, D.C. 20016, USA
[3]The Catholic University of America, Department of Physics, Washington, D.C. 20064, USA
[4]Computer Sciences Corporation, Laurel, Maryland 20701, USA
[5]U.S. National Museum of Natural History, Smithsonian Institution, Department of Mineral Sciences, MRC-NHB, Washington, D.C. 20560, USA
[6]University of Arizona, Lunar and Planetary Laboratory, Tucson, Arizona 85721, USA
[7]Max Planck-Institut für Chemie, Abteilung Kosmochemie, Saarstrasse 23, D-52122 Mainz, Germany
[8]Harvard Smithsonian Astrophysical Observatory, 60 Garden Street, Cambridge, Massachusetts 02138, USA
[9]Cornell University, 528 Space Science Building, Ithaca, New York 14853, USA
[10]Los Alamos National Laboratory, Mail Stop D436, Los Alamos, New Mexico 87545, USA
[11]Johns Hopkins University Applied Physics Laboratory, Laurel, Maryland 20707, USA
[12]University of California, Berkeley, Berkeley, California 94702, USA
*Correspondence author's e-mail address: u1jit@lepvx3.gsfc.nasa.gov

(Received 2001 August 21; accepted in revised form 2001 October 19)
(Part of a series on the Near–Shoemaker mission to 433 Eros)

Abstract–The near-Earth asteroid rendezvous (NEAR)–Shoemaker remote-sensing x-ray/gamma-ray spectrometer (XGRS) completed more than a year of operation in orbit and on the surface of 433 Eros. Elemental compositions for a number of regions on the surface of Eros have been derived from analyses of the characteristic x-ray and gamma-ray emission spectra. The NEAR XGRS detection system was included as part of the interplanetary network (IPN) for the detection and localization of gamma-ray bursts (GRBs). Preliminary results for both the elemental composition of the surface of Eros and the detection of GRBs have been obtained. In addition to the science results, the design and operation of the NEAR XGRS is considered. Significant information important for the design of future remote sensing XGRS systems has been obtained and evaluated. We focus on four factors that became particularly critical during NEAR: (1) overall spacecraft design, (2) selection of materials, (3) increase of the signal-to-noise ratio and (4) knowledge of the incident solar x-ray spectrum.

INTRODUCTION

Passive remote-sensing x-ray and gamma-ray spectroscopy (XGRS) has been used to obtain elemental composition maps of planetary bodies since the earliest days of space exploration. The Apollo 15 and 16 missions (Adler *et al.*, 1972; Fichtel and Trombka, 1997; Evans *et al.*, 1993; Yin *et al.*, 1993; Boynton *et al.*, 1993) and the Lunar Prospector mission (Feldman *et al.*, 1996; Lawrence *et al.*, 1998) carried orbital gamma-ray and x-ray spectrometers to determine the surface composition of the Moon. A major accomplishment of this work was the recognition of the highlands/mare compositional trichotomy and the diversity of basalt compositions within the mare (Jolliff *et al.*, 2000). Gamma-ray spectroscopy continues as an important tool for the future of Mars exploration, with the *Mars Odyssey 2001* spacecraft (Boynton *et al.*, 2000).

Measurements of discrete-line x-ray and gamma-ray emissions by spacecraft from orbit and on the surface of planetary bodies provide quantitative elemental surface analyses. X-ray spectroscopy can be applied to bodies with no significant atmosphere, where the x-ray spectrum from the surface is dominated by a combination of solar x-ray induced fluorescence and coherent and incoherent scattered solar x-rays. Sampling depth is dependent on energy, but is <100 μm for elements that can be detected. This represents the uppermost layer of regolith and is comparable to the optical regolith sampled by reflectance spectroscopy. The technique is limited to detection of major and a few minor elements, including Mg,

Prelude preprint MS#4631

Al, Si, S, Ca, Ti and Fe. In order to obtain quantitative results, detailed knowledge of the incident solar x-ray flux is required.

Gamma-ray emission can be observed from bodies that have no significant magnetic field and a low atmospheric density. Gamma-ray lines are attributed to the natural radioactive isotopes and daughter products of K, Th, and U, and to cosmic-ray primary and secondary particle-induced activation, primarily of the major elements H, C, N, Fe, O, Si and Mg. Elemental composition to ~10 cm below the surface can be determined.

The near-Earth asteroid rendezvous (NEAR)–Shoemaker XGRS system (Trombka *et al.*, 2000a,b) completed a year of operation in orbit around and on the surface of 433 Eros. In a series of companion papers, we describe the methods for analyzing these data and comparing them to meteoritic compositions, the results and interpretations of the x-ray and gamma-ray spectrometers individually, and the synthesis of these data with results from the multi-spectral imager/near-infrared spectrometer experiments (Nittler *et al.*, 2001; Evans *et al.*, 2001b; McCoy *et al.*, 2001). In this paper we focus on the instrumentation itself to give the reader a brief overview of the design, capabilities and limitations of these instruments, an overview of results from the NEAR XGRS experiment, and some thoughts on the design of instrumentation for future missions.

TIMING AND LIMITATIONS ON OBSERVATIONS

The *NEAR–Shoemaker* spacecraft was launched from Cape Canaveral on a Delta-2 rocket on 1996 February 17 for a planned rendezvous with asteroid 433 Eros in December of 1998. On 1997 June 7, a flyby of the asteroid Mathilde was carried out and images of the asteroid were obtained (Veverka *et al.*, 1997). The *NEAR–Shoemaker* spacecraft initiated an Earth swingby on 1998 January 23 to put it on its course for rendezvous with the asteroid Eros. The initial Eros rendezvous maneuver was aborted on 1998 December 23 when contact with the spacecraft was interrupted but reestablished after 27 h of silence. The *NEAR–Shoemaker* spacecraft came within 3827 km of Eros during the flyby, but this was not close enough to obtain statistically significant XGRS data. Because of the abort, the rendezvous was delayed by over 1 year. During the month of December 1999 the *NEAR–Shoemaker* spacecraft was integrated into the interplanetary network (IPN) for the localization of gamma-ray bursts. NEAR entered Eros orbit on 2000 February 14 at the start of a 1 year orbital mission. During this period orbits ranged from circular to elliptical, at distances from the center of mass of the asteroid from 200 to 35 km. NEAR completed a successful controlled descent to the surface of Eros on 2001 February 12.

Although the XGRS system was observing 433 Eros during the entire 1 year orbital period, there were a number of time periods during which the XGRS team controlled spacecraft pointing. Compositional data were collected over a range of orbits, and the first x-ray signal from the surface of Eros was detected while NEAR was still in a 100 km orbit (Trombka *et al.*, 2000b). The best quality compositional data were acquired during low altitude orbits. The optimum periods for orbital observations were 2000 April 30 to 2000 July 6, when the spacecraft was in an almost circular 50 km orbit; 2000 July 7 to 2000 August 25, in both circular and elliptical orbits starting at 50 to 35 km; and 2000 December 13 to 2001 January 23, when we were in an almost circular 35 km orbit. Upon landing on 433 Eros on 2001 February 12, the gamma-ray spectrometer obtained *in situ* measurements of the regolith for a period of ~14 days.

Although the period of orbital observations controlled by the XGRS team totaled almost 6 months, the period of useful data collection for each instrument was considerably shorter. This resulted primarily from the fact that *NEAR–Shoemaker* was a fixed-body spacecraft, and thus observations of specific targets on the surface of 433 Eros required pointing the entire spacecraft. Targeted pointing was severely limited by constraints on time for telemetry to Earth (~8 h/day), and the restriction that the solar panels had to be within ±30° of the normal direction to the Sun. Moreover, x-ray measurements required that the portion being observed be in sunlight, and that solar incidence and fluorescence emission angles be within 60° of normal. In practice, off-nadir pointing was required to simultaneously satisfy most of these criteria. Finally, as discussed in detail by Nittler *et al.* (2001, unpubl. data), the solar spectrum, which is the excitation source for fluorescence from the surface of the asteroid, changes dramatically on short timescales. The highest quality x-ray data are acquired during periods of solar flares, both because the overall solar flare is higher, and because spectral hardening (*i.e.*, the higher energy x-rays increase relative to the lower energy) leads to enhanced emission of higher Z elements (*e.g.*, Fe). Although there were a significant number of solar flares during mission operation, the total number of flares that occurred during optimal viewing conditions was quite low.

Orbital gamma-ray observations were much more restricted in terms of time. In orbits at 50 km and above, the asteroid effectively filled only a small portion of the field of view and the background overwhelmed the signal from the surface. Even during 35 km orbits, the signal-to-noise ratio was very poor for detection of gamma rays from the asteroid. Although we believe these data may ultimately be reduced to yield meaningful results, we have focused our initial efforts (Evans *et al.*, 2001b) on the *in situ* gamma-ray data collected at the end of the mission. Since signal intensity scales as the square of distance from the target, the signal-to-noise ratio of these data is an order of magnitude better than even the low altitude orbits.

INSTRUMENTATION

Goldsten *et al.* (1997), Trombka *et al.* (1997, 2000a), Evans *et al.* (2000), Starr *et al.* (2000) describe the NEAR x-ray and gamma-ray detector systems in detail, and here we give a brief

summary. The NEAR XGRS system is a non-dispersive spectroscopic system. In this approach the incoming x-ray or gamma-ray photon is absorbed by the detector material, and a voltage pulse proportional to the energy absorbed is measured at the detector output. An analog to digital conversion is then performed and the count is binned by "pulse height" or energy loss. The obtained spectrum is telemetered to Earth. From an analysis of the pulse height spectrum elemental composition can be inferred. In order to understand the design and operation of the XGRS system, a brief discussion of the nature of spectral measurement of x-rays and gamma rays as expressed in the pulse height spectrum and of the space background is presented.

As mentioned above, the pulse height spectrum reflects the amount of energy that is lost in the detector and transferred as kinetic energy to the electrons in the detector. Thus the measured spectrum is not in a one-to-one correspondence with the true incident spectrum. For example, the measured pulse height spectrum for monoenergetic gamma rays or x-rays is never just a single line feature. Rather, its shape is determined by such factors as the relative magnitude of the major interaction processes, which include photoelectric absorption, Compton scattering and pair production, and the losses and statistical fluctuations that characterize the detector system. First, consider the shape of the response of a detector to monoenergetic gamma rays or x-rays at lower energies where photoelectric absorption predominates. In this case an incoming photon knocks out a bound electron, and the kinetic energy lost to the electron is equal to the energy of the incoming photon minus the binding energy of the electron in its particular shell (*e.g.*, K shell). After the interaction has taken place, the atom is left in an excited state. An x-ray with energy equal to the binding energy can then be emitted. This binding energy may be reclaimed by the absorption of this x-ray, but in some cases the x-ray can escape the detector without absorption. The monoenergetic pulse height spectrum as measured would be composed of a total absorption peak called the "photopeak" and a second, usually smaller lower energy peak, known as the "escape peak".

The second process, Compton scattering, is similar to billiard ball scattering in that the photon collides with an unbound electron, loses some of its energy to the electron, and then scatters away in another direction with a decreased energy. Not all of the photon energy can be lost in the Compton scattering process. When Compton scattering becomes an important energy-loss mechanism, another region is observed in the pulse height spectrum, called the Compton continuum. All the energy lost in Compton scattering is given up to the electron as kinetic energy. The gamma ray may lose part of its energy to the detector and escape the crystal, suffer further scattering and either escape the crystal, or be completely absorbed by the photoelectric absorption process. The Compton continuum region adds to the background continuum and thus decreases the signal-to-noise ratio.

The third process, pair production, becomes possible at energies above 1022 keV. A positron-electron pair can be created as part of the photon-detector interaction. The total energy minus 1022 keV (the rest mass of the electron-positron pair) is imparted as kinetic energy to the electron and positron pair. The electron usually loses its kinetic energy near the pair production site, while the positron, after losing its kinetic energy to the detector annihilates with an electron, producing two gamma rays each with 511 keV energy. The energy of these gamma rays can either be absorbed in the detector or can escape. Therefore, in this energy region three peaks will be seen in the pulse height spectrum: (1) pair production with escape of both annihilation quanta (double escape peak); (2) pair production with the absorption of one annihilation quantum (single escape peak); and (3) total absorption by any method (photopeak). Photoelectric absorption is the dominant process for the x-ray region of interest in the XGRS system. In contrast, all three processes are of importance for the gamma-ray spectrometer.

The XRS package included three asteroid-pointing detectors for surface studies in the 0.7–10 keV energy region, and two detectors to monitor the Sun that were oriented at 90° relative to the asteroid-pointing ones. Figure 1 is a schematic drawing of the asteroid-pointing detector system. The asteroid-pointing detectors were sealed gas-filled proportional counters. Their energy resolution measured both in the laboratory and in flight was 14.5% at 5.9 keV. Balanced filter systems were used to separate the overlapping lines of Mg, Al, and Si. A honeycomb-design collimator composed of copper with 3% beryllium over the asteroid-pointing detectors limited the field of view to 5° to reduce sky background and to improve spatial resolution. A 5° field of view yields a spatial resolution of ~4.4 km at a distance of 50 km from the surface of the asteroid. We remind the reader that orbital distances are from the center of mass, not from the surface of the asteroid. The solar-pointing detector that was used during orbital measurements of Eros was also a proportional counter similar to the surface detectors, but with a graded filter that allowed measurement of the solar x-ray emission spectrum over intensities that can vary 5 orders of magnitude. The other solar-pointing detector was a Si positive-intrinsic-negative (PIN) solid-state detector. Three ^{55}Fe calibration sources were included to establish the energy calibration for each of the asteroid-pointing detectors. X-ray spectral measurement times could be varied from 1s to 18 h. During <50 km orbits, the integration time was set to 50 s. All x-ray pulse height spectra were binned into 256 channels covering the range of ~0.7 to 10 keV. Cosmic rays typically produce electronic pulse height signals in proportional counters with longer rise times than the x-ray signal. Above ~2 keV, the rise time difference was large enough to be electronically discriminated. Thus for the higher energy portion of the pulse height spectrum, rise time discriminators were used to decrease the cosmic-ray background.

The NEAR gamma-ray spectrometer utilizes a NaI(Tl) detector with a bismuth germanate ($Bi_4Ge_3O_{12}$ or BGO) active collimator. NaI(Tl) was chosen because it has the best energy

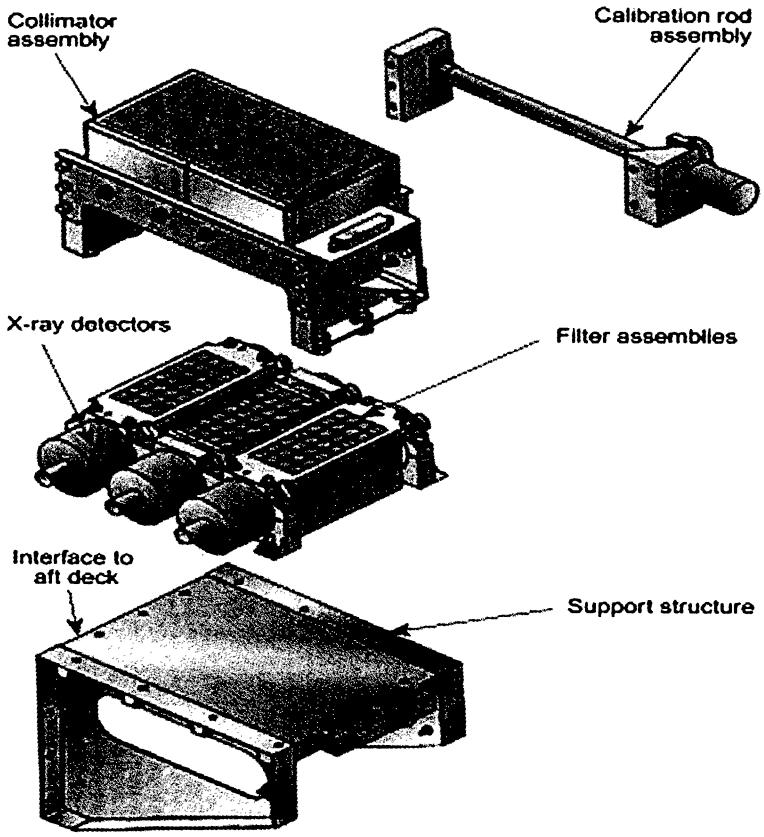

FIG. 1. Schematic drawing of the NEAR x-ray spectrometer.

resolution for scintillation detectors in combination with photomultiplier tubes. These systems are rugged and have been used successfully in many space-flight missions. Unlike previous missions, the gamma-ray detector for the NEAR mission was mounted on the spacecraft. Without shielding, the background produced by the cosmic-ray activation of the spacecraft materials would significantly degrade the orbital and surface measurements. A further major source of background was caused by the direct interactions of cosmic rays in the central detector. The active collimator is needed to reduce these two major background components. The active shield detects a simultaneous interaction in the shield and detector and inhibits the measurement of the event in the central detector. BGO, with a density of 7.13 g/cm^3, was chosen for the NEAR GRS collimator. The high-purity Ge GRS on the 2004 Japanese SELENE orbital mission to the Moon also will be body mounted, and will use a large shield of BGO between the Ge and the spacecraft (Hasebe *et al.*, 1999).

The active BGO shield also is useful in reducing the partial absorption gamma-ray events in the central detector by the so-called "Compton suppression method". However, some significant information can be lost when an active shield is used. For example, the first and second escape peaks produced as a result of pair production interactions in the central scintillator will be greatly reduced in the anticoincidence spectrum since either one or two 511 keV gamma rays escape the central detector and can be detected simultaneously in the shield detector. The first and second escape peaks would thus be rejected in the anticoincidence spectrum. At energies greater than ~2 MeV, pair production becomes an important cross-section for the absorption of these higher energy gamma rays. For a small central detector like the NEAR design, this loss of signal would be unacceptable since the first and second escape peaks are larger than the photopeak for many gamma rays of interest. Fortunately, this information can be recovered by collecting two additional coincidence NaI(Tl) spectra. These coincidence spectra include all events in the central detector that occur simultaneously with deposition of 511 or 1022 keV (*i.e.*, the sum of two 511 keV) in the BGO.

Figure 2 is a cross-section view of the gamma-ray flight detector system. The central scintillator is the prime detector and is a 2.54 × 7.62 cm right circular cylinder NaI(Tl). A 2.54 cm diameter metal ceramic photomultiplier is used in combination with the NaI(Tl) scintillator. The shield detector is a BGO cup with an outside dimension of 8.9 × 14 cm. A 7 cm diameter metal ceramic photomultiplier is used in combination with the BGO. The energy resolution at 661keV is 8.7% and 14% for the NaI(Tl) and the BGO shield, respectively. The energy range

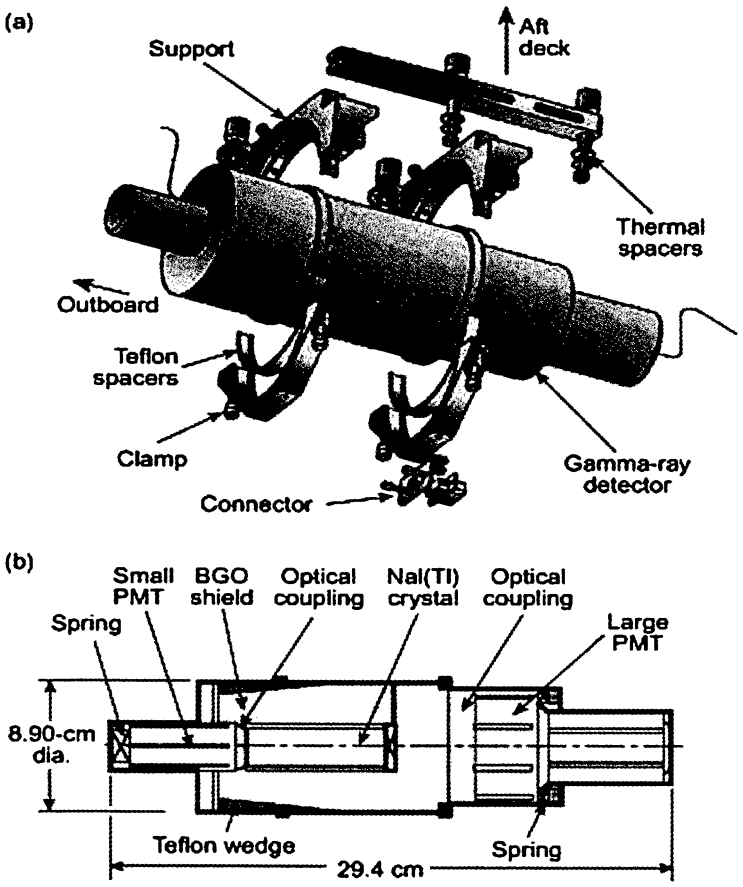

FIG. 2. Schematic drawing of the NEAR gamma-ray spectrometer.

for both detectors is 0.1–10 MeV. Five pulse height spectra are obtained with the gamma-ray spectrometer system. These are the NaI(TI) raw spectrum (without either coincidence or anticoincidence); the BGO raw spectrum; the NaI(Tl) spectrum in anticoincidence with BGO; the NaI(Tl) spectrum in coincidence with the BGO 0.511 MeV line; and the NaI(Tl) spectrum in coincidence with the BGO 1.022 MeV line. The nominal integration time for the GRS system was 1200 s, although it could be varied from 1 s to ~18 h. Details of the design of the detector systems can be found in Trombka *et al.* (1997) and Goldsten *et al.* (1997).

SUMMARY OF SCIENTIFIC RESULTS

The primary mission of NEAR was to investigate the mineralogy, composition, magnetic fields, geology and origin of 433 Eros. The results of these investigations, from the perspective of the XGRS instrument, are presented in this volume by Nittler *et al.* (2001), Evans *et al.* (2001b) and McCoy *et al.* (2001). Thus, we review these only briefly in this paper. The gamma-ray spectrometer on the *NEAR–Shoemaker* spacecraft was also used to detect gamma-ray bursts. Jensen *et al.* (2001), Klose *et al.* (2000), Hurley *et al.* (2000), and Anderson *et al.* (2000) review some of the results of this effort in detail. We present these results in this paper to familiarize readers with the full range of capabilities and scientific utilities of this suite of instruments.

Elemental Composition of 433 Eros

The surface composition of 433 Eros measured during quiet Sun and solar flare conditions by XRS and during *in situ* measurements by GRS suggests that Eros is similar in bulk composition to a range of meteorites that have experienced minimal thermal alteration since their formation at the birth of the solar system. Certainly, Eros is broadly "primitive" in its chemical composition and has not experienced global differentiation into a core, mantle and crust. Differences between XRS and GRS in Fe/Si ratio (Evans *et al.*, 2001b) and an apparent deficiency of sulfur at the surface of Eros (Trombka *et al.*, 2000b; Nittler *et al.*, 2001) could reflect either alteration processes in the regolith during the last millions to billions of years or partial melting in the first 10 Ma of solar system history. The GRS results reported by Evans *et al.* (2001a) are only for

a volume of ~1 m^3 at the spacecraft's landing site on the surface of Eros, which appears to be at the edge of one of the smooth "ponds" seen in the descent images. The orbital GRS data have a very weak signal from Eros (Evans *et al.*, 2001a), but a very careful analysis of the orbital GRS data could yield global abundances of a few key elements such as iron.

Gamma-Ray Burst Detection

Gamma-ray bursts (GRBs) are flashes of high-energy photons occurring typically about once a day somewhere in the sky. Their origins remain a mystery to astronomers, who generally agree that GRBs are enormous explosions that occur throughout the universe. Only recently has enough evidence been culled to link the longest of these bursts to hypernovas: giant, extraordinarily intense, unusual supernovas, dying stars that collapse under their own weight. At their peaks, these bursts are by far the brightest emissions of gamma-ray radiation in the sky. In fact, GRBs are the most powerful explosions in the known universe, generating more energy in a few seconds than the Sun will generate in its entire lifetime. Recent data indicate that these bursts are of cosmological origin (Jensen *et al.*, 2001; Klose *et al.*, 2000).

In order to understand better the nature of GRBs, it is important to determine their position in the sky and to see if these objects can be associated with sources that have been observed in other parts of the electromagnetic spectrum. The IPN has been established to localize GRBs by timing their arrival at different distant spacecraft. The IPN benefited greatly from the inclusion of NEAR in the network over a 15 month period from December 1999 to February 2001. During this period, the network included NEAR, *Ulysses*, *GGS-Wind* (the Konus instrument), *BeppoSAX* (the gamma-ray burst monitor), and the *Rossi* x-ray timing explorer (the All Sky Monitor). With NEAR in the network over 100 GRBs were detected. Of them, 34 were localized rapidly enough and precisely enough to allow optical and radio follow-up observations. That is, the locations were determined within ~24 h, and the positions were derived with accuracies of the order of several arcminutes. These radio and optical observations resulted in the discovery of nine new counterparts, and of the nine, distances were obtained for five of them by measuring their redshifts. (These numbers represent increases of ~50% to the database of GRB counterparts.) The most interesting result was the detection of a burst originating in the southern constellation Carina, which, with a redshift of 4.5, is the most distant GRB yet detected. The gamma radiation traveled for 12.5 Ga before being detected by the network (Anderson *et al.*, 2000).

LESSONS FOR FUTURE MISSIONS

Cost constrained missions such as those represented by the NEAR mission present significant challenges to the team of engineers and scientists involved in project development and operation. On the positive side, the NEAR mission experience has demonstrated the importance of the strict discipline needed in planning and operation to maintain cost-effective projects. On the other hand, the cost constraints on these early missions have limited our ability to build in sufficient contingency capabilities. This mission was the first with fixed solar panels to orbit around a non-spherical body. It was difficult to accommodate the differences projected in the planning prior to launch with the actual low orbital profile. Further, when the mission slipped a year the mission profile changed, and for the NEAR XGRS system, the time and quality of observations was changed significantly, posing a risk to the return of scientific results. Finally, the shortness of both time and funding available between the initiation of the mission and launch limited our ability to complete the calibration of the flight detector systems for any conditions other than those planned for the original mission profile. This has complicated our post-mission analysis procedures.

As a result of the experience gained with the NEAR XGRS and from flights of remote-sensing XGRS experiments on *Apollo*, *Lunar Prospector*, *Mars Observer*, *Mars Odyssey 2001* and *WIND* transient gamma-ray spectrometer (TGRS) (Owens *et al.*, 1995) a number of lessons have been learned concerning the design, flight operation and data analysis of such systems. We consider the gamma-ray and x-ray experiments separately and focus on the factors that became particularly critical during the NEAR mission.

The gamma-ray detector was very constrained on the NEAR mission. NEAR differed significantly from previous missions in being a spacecraft without booms for extending instruments from the spacecraft body or the ability to point individual instruments independently from the spacecraft body. The boom system deployed on previous missions allowed for a significant reduction in background and increase in signal-to-noise ratio for the gamma-ray spectrometer. In the Apollo system, the solid angle subtended at the detector by the spacecraft was <10% of the solid angle subtended by the detector and the measured area on the surface of the Moon. During the orbital phase of the NEAR mission, the surface of 433 Eros never subtended a solid angle of greater than ~0.1π steradians, whereas the spacecraft subtended just under 2π steradians. This made it necessary to design a more complex gamma-ray detector with an active shield to help compensate for the large signal from the spacecraft. The efficiency of the shield in reducing the spacecraft background was quite energy dependent, and at energies above ~2000 keV, only a factor of two reduction was achieved. The size of the central detector and the shield was limited by mission mass constraint. As a consequence, even with the active shield, the spacecraft background was an order of magnitude higher than the observed emission from the surface of the asteroid. Things greatly improved once NEAR had landed on the surface of Eros when a ~π steradians solid angle was achieved. Moreover, the flux of cosmic rays on the detector was decreased by almost a factor of 2 on the surface compared to orbit.

Clearly, the most effective means for reducing background is using booms. If such booms are not possible, in missions such as NEAR and SELENE, active shields can be used, but they must be large enough to produce a significant background reduction relative to the expected solid angle subtended by the remotely sensed solar system body.

Planetary exploration missions impose severe constraints on the size, mass (typically 5 to 10 kg) and power (10 kW) available for the scientific payload. Furthermore, these missions may last 2–10 years and, in many cases, the first measurement of the planetary surface may not be made until 2–7 years after launch. The effects of long-term solar cosmic rays, galactic cosmic-ray and high-energy electron-exposure effects must be taken into consideration when selecting materials used in the detector package. As noted earlier, we compensated for the fixed-body nature of the NEAR gamma-ray spectrometer by including an active shield of bismuth germanate. However, the selection of bismuth germanate had an unexpected consequence. We observed a 2.61 MeV line in data returned from NEAR, which is where we would expect the strongest gamma-ray line for the radioactive element Th. Although we did not observe this as a significant line in the background during ground-based testing, we now believe that this 2.61 MeV line was produced by high-energy proton and neutron interactions in ^{209}Bi (a component of the bismuth germanate shield) yielding the radioactive element ^{208}Tl. This isotope decays with a 3.05 min half-life to ^{208} Pb by beta emission and yielding the 2.61 MeV line (Lederer and Shirley, 1978). This background limits the sensitivity for detection of Th.

Another problem with induced activity became apparent when the surface measurements were obtained. Figure 3 shows the orbital and surface pulse-height anticoincidence spectra. The surface spectrum shows a considerable increase in the background in the lower energy domain up to ~2 MeV compared with the orbital spectrum. This enhancement can be attributed to the activation of ^{128}I in the NaI(Tl) detector. This component can be seen in the surface spectrum because of the large relative increase of the thermal neutron flux on the surface relative to that observed in orbit. These examples underscore the problems in the selection of materials used in the detector and surrounding packaging materials that must be considered when designing a detector system.

An increased signal-to-noise ratio would greatly improve future remote-sensing gamma-ray experiments. The NEAR gamma-ray spectrometer had a lower signal-to-noise ratio than the two previous successful uses of remote gamma-ray sensors; Apollo and Lunar Prospector. This reflected the fact that the latter missions used booms, whereas the NEAR mission was such that a much smaller solid angle was subtended compared to the lunar missions, and that Eros is apparently quite spatially homogeneous in composition. Elemental variations on the Moon are quite dramatic and hence easier to map. Missions having constraints similar to the NEAR mission will require detailed simulations of the orbital operations after the object's shape has been determined. In many cases, the shape may be determined only after early measurements in orbit. Once these simulations are completed, orbital operations may have to be significantly modified relative to the preflight and early in-flight planning.

Better energy resolution can significantly improve the detection efficiency of a gamma-ray system. Figure 4 shows measurements of the same soil sample using both the NEAR

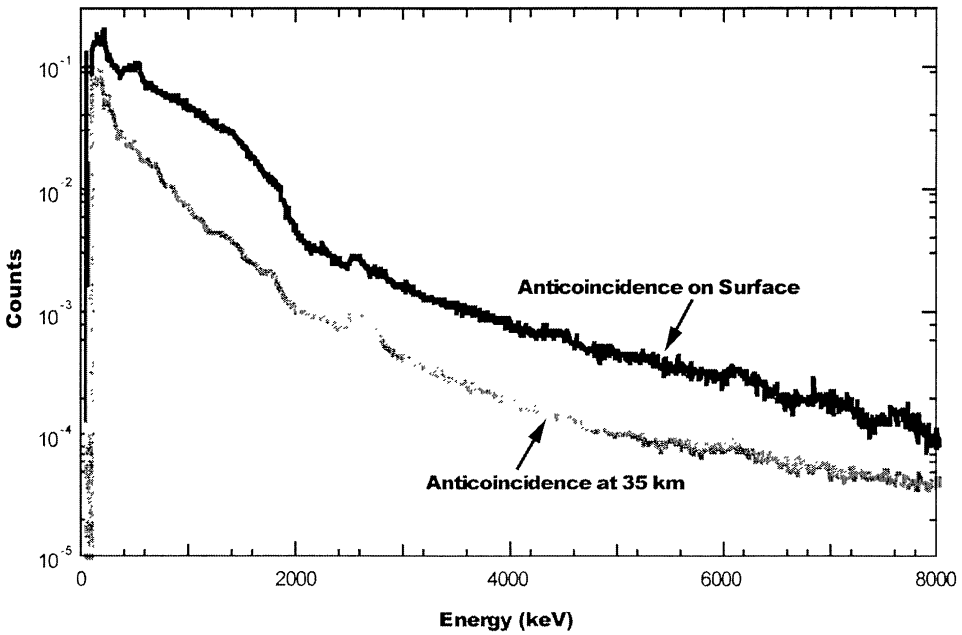

FIG. 3. Comparison of the NEAR gamma-ray orbital and surface anticoincidence pulse height spectra.

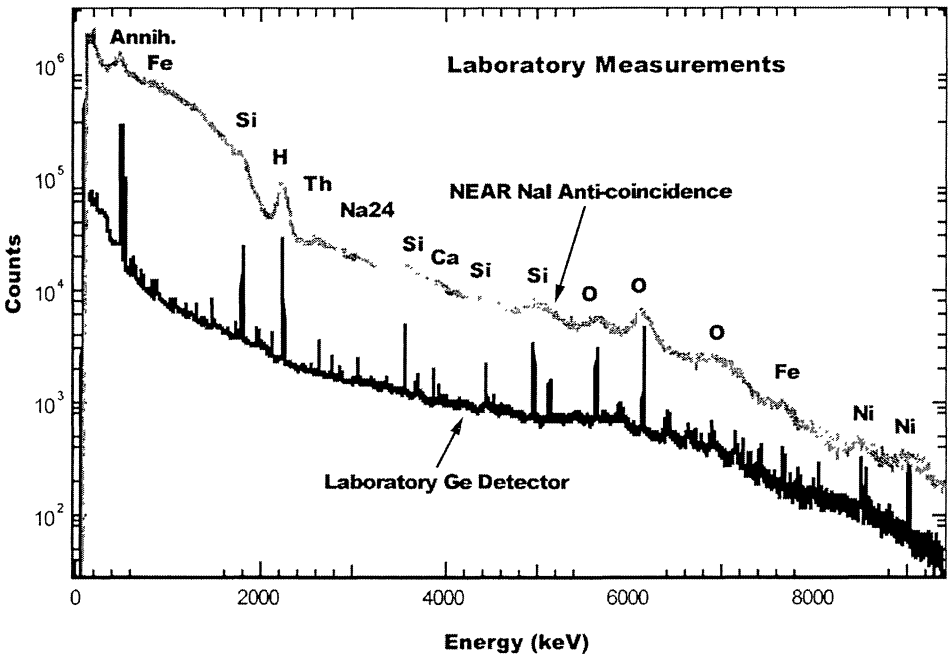

FIG. 4. Comparison of NEAR gamma-ray pulse height spectrum with a Ge pulse height spectrum using a soil sample and a 14 MeV generator excitation source to simulate the space environment.

scintillation detector system and a Ge detector. The elemental composition is determined by analyzing the intensity of the discrete line emissions. The relative improvement in signal-to-noise can be seen in the shape and width of the lines relative to the background. No matter the resolution, the peak efficiency must be high enough to see the peaks over the background. In Fig. 5, the BGO and the NaI(Tl) escape spectra are shown. The poorer energy resolution BGO scintillation counter still can detect the lower energy lines of Fe, K, and Si above a rather high background. The higher energy lines of O also can be seen.

The energy resolution of the Ge detector is more than an order of magnitude better than scintillation detectors. However, Ge detectors require operation at cryogenic temperatures, which could not be accommodated on the NEAR mission. The problems of long-term operation of Ge in the space environment and the requirement of continuous cryogenic operation may limit their use on future space-flight missions. Recent results from the many years of space operation of the *Wind* TGRS (Kurczynski *et al.*, 1999) experiment launched in November 1994 has supplied important information on the operation of such detectors in the space environment for over 4 years. Significant information can be obtained with both Ge and scintillation detectors. Of course, in addition to improved signal-to-noise, the better the energy resolution, the more sensitive the system is to large ranges of elemental composition, given good peak detection efficiencies. A number of room-temperature solid-state detectors with better energy resolution are under development, such as CdZnTe, and should be available for future space-flight missions. These detectors can be more easily maintained at or near room temperature with less power and weight than those that attempt to cool to cryogenic temperatures. The choice of the detector system therefore depends on mission profile and other mission constraints.

We now consider the x-ray spectrometer. As mentioned, the NEAR mission represents the second time this system design was used for elemental composition measurements of solar system bodies. The first measurements were carried out during the Apollo 15 and 16 missions (Adler *et al.*, 1972; Yin *et al.*,1993). The Apollo measurements were carried out during solar minimum and only data for the relative composition of Mg, Al, and Si were obtained. The balanced filter technique was used with gas proportional detectors (Adler *et al.*, 1972; Yin *et al.*, 1993). There were a number of significant differences between the Apollo and NEAR missions. As for the gamma-ray spectrometer, the solid angle subtended by the detector on the Apollo missions was significantly greater than that achievable on the NEAR mission. The Apollo mission operated at 1 AU from the Sun while the *NEAR–Shoemaker* spacecraft was operated at about an average 1.4 AU from the Sun with a consequent drop in solar x-ray flux. Operating NEAR during solar maximum did partially offset the decrease in solar x-ray flux since the intensity of x-ray emission even during quiescent periods is higher during solar maximum than during solar minimum.

A major source of background in the proportional counters is due to cosmic-ray interactions with the gas. As discussed

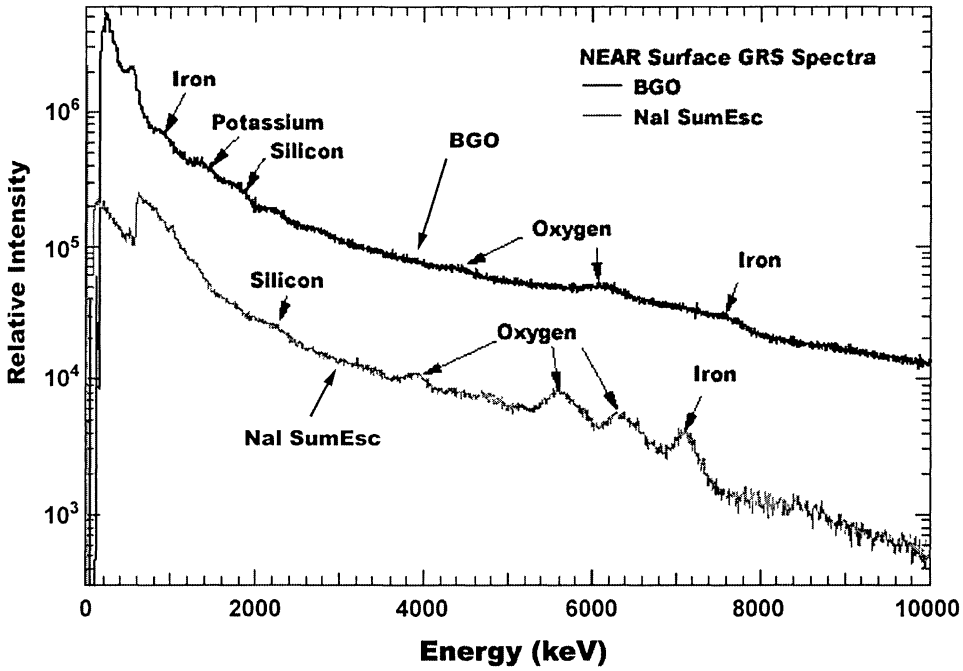

FIG. 5. Surface gamma-ray pulse height spectra for both the BGO detector and the NaI(Tl) detector. The NaI(Tl) spectrum is the escape spectrum.

above, rise time discrimination can in principle distinguish between charged particles and x-rays and such system were used during both the Apollo and NEAR missions (Adler *et al.*, 1972; Goldsten *et al.*, 1997). An order of magnitude reduction in cosmic-ray background was achieved with the Apollo detector in the 1 to 3 keV region, but because of design constraints, this reduction was only possible above ~2 keV in the NEAR system (Goldsten *et al.*, 1997). Thus, the signal-to-noise ratio in the spectral region corresponding to Mg, Al, and Si was lower for the NEAR system, and measurements during quiescent solar activity periods required significantly longer integration times as compared with the Apollo system.

On future space-flight missions, reduction of this background component is of prime importance. Such reduction could be achieved in a number of different ways. Rise time discrimination or internal guard wires can be used in proportional counters. The NEAR proportional counters had a single wire to collect charges generated by the energy-loss trajectory of particles and photons in the detector. By using multiple (guard) wires, one can reconstruct the energy-loss trajectory of particles and photons in the detector. Cosmic rays produce events on longer tracts in the counter and hence can be discriminated against. Active cosmic-ray shields similar to the approach used for the gamma-ray systems also have proven effective. Finally, the use of large area room-temperature solid-state detectors could be effective, because cosmic rays produce a much lower background in these detectors compared with proportional counters in the pulse height region of interest for XRS. This was observed during the early cruise phase of the NEAR mission and will be discussed below. The importance of reducing the background cannot be overemphasized. Reducing the background allows shorter integration times and thus better spatial surface mapping.

Finally, accurate knowledge of the incident solar spectrum is needed in order to deduce elemental concentration ratios and abundances. Small variations in the determination of the shape of the incident solar spectrum may yield rather large differences in the elemental abundances derived from the measured photon ratios (Nittler *et al.*, 2001). Two methods have been proposed for monitoring the solar x-ray flux. In the first case, a standard sample aboard the spacecraft whose elemental composition is well determined could be used. Then measurements of the solar x-ray produced fluorescence spectrum from the sample would be used for calibration. This is the equivalent of using standards in laboratory x-ray fluorescence measurements.

A second method is to monitor the solar x-ray spectrum directly. The problem with the first method is that a separate, complete XRS system would be required since simultaneous monitoring is required, and both volume and weight constraints would likely prevent such redundant systems from being included on planetary missions. Thus the direct observation of the solar emission spectrum was used on Apollo and NEAR, and seems most promising for future missions.

Accurate monitoring of the solar x-ray spectrum has been rather difficult to achieve. There are a number of problems.

First, both the continuum and the large number of discrete line emissions must be well determined, requiring high-resolution detectors. Such detectors previously have not been available to measure these spectra over the energy domain of importance (*i.e.*, from ~1 to ~10 keV). Recent studies indicate the feasibility of including such detectors of future space-flight missions. Second, during solar flares the intensity can change by up to 5 orders of magnitude over a very short time, and a very high dynamic range is thus needed for the detector system. On Apollo, only quiet Sun data were analyzed and a proportional counter with a pin hole aperture was used as a solar monitor. The NEAR mission operated during solar maximum when the Sun was more active than during Apollo. The most important observations were made during solar flare periods, and elemental compositions of the higher atomic number elements (up to Fe) were obtained.

As described earlier, two different solar monitor detectors were included aboard the *NEAR–Shoemaker* spacecraft: a proportional counter with a special filter that allowed operation over 4 decades of flux intensity change (Clark *et al.*, 1995); and a room-temperature Si PIN detector with a pinhole aperture and Be filter, which also allowed operation over 4 decades of flux change. The energy resolution for the proportional counter was ~850 eV for the ^{55}Fe (5.9 keV) line and the Si PIN detector energy resolution was ~649 eV for the same line. The Si PIN detector was included for test purposes and as a possible backup to the proportional counter. Rise time discrimination was not used to reduce the cosmic-ray background in the solar pointed proportional counter.

Figure 6a shows solar spectra measured during a quiet Sun period obtained using the proportional counter and the Si PIN detector, and Fig. 6b shows the spectra obtained during a solar flare. The cosmic-ray background dominates the quiet Sun solar spectrum measurement using the proportional counter, while the Si PIN detector has a very small contribution from the cosmic-ray background. We believe that the reason for this is that the cosmic-ray events produce most of their pulses above the upper discriminator level and are therefore rejected. The improved energy resolution of the Si PIN detector also produces better spectral measurements during solar flares. Unfortunately, the Si PIN detector could not be used during orbital operation because of several space environment problems (Starr *et al.*, 1999). First, space charge effects due to both high-energy electrons and cosmic rays caused the detector to cease operation for long periods of times before recovery. The detector also suffered radiation damage effects due to the long exposure to the space radiation environment. We therefore had to depend on the proportional counter solar monitor during orbital operation. A major problem with the NEAR proportional counter detector can be attributed to the special filter used. The lower energy portion of the spectrum was greatly degraded, and the response was very sensitive to the orientation of the detector with respect to the incident solar flux. Unfortunately, the energy response of the graded filter was not measured prior to flight, and data analysis has hence relied on modeling, which is subject to many important uncertainties (Nittler *et al.*, 2001).

For future missions, we believe that if proportional detectors are used, a guard wire system should be used to decrease cosmic-ray induced background. We also believe those room-temperature detectors such as PIN and drift Si and PIN CdTe will be available once the problems of space charge and space radiation damage are better understood. We further believe that a double detector design should be used. One detector would measure the quiet Sun and lower intensity flare, and the other would measure the higher intensity solar flares. This would allow for a simpler filter design, would improve detection efficiency and would be less sensitive to solar x-ray flux incidence angle. Laboratory calibrations of all detectors and filters are also absolutely essential.

Acknowledgments–We wish to thank the NEAR project offices at both Johns Hopkins University/Applied Physics Laboratory (J.H.U./A.P.L.) and NASA Headquarters. The NEAR mission is supported by NASA Task 005 NASA Contract NAS 5-97271, by NASA contract 624-03-03 and by the Planetary Instrument Development and Design Program under NASA contract 344-96-30. The XGRS Team also recognizes the exemplary efforts of the NEAR Mission Operations Team, the NEAR Navigation teams at J.H.U./A.P.L., J.P.L., and the Deep Space Network and the NEAR Science Data Center at J.H.U./A.P.L. for enabling the collection of the data that has made this analysis possible. We wish to thank the student support at Cornell University, the University of Arizona and NASA Goddard Space Flight Center. We wish to express our great appreciation to Pam Solomon for her invaluable technical assistance in the preparation of this paper.

Editorial handling: D. W. G. Sears

REFERENCES

ADLER I., TROMBKA J. I. AND GORENSTEIN P. (1972) Remote chemical analysis during the Apollo 15 mission. *Anal. Chem.* **44**, 28a–35a.

ANDERSON M. *ET AL.* (2000) VLT identification of the optical afterglow of the gamma-ray burst GRB000131 at Z = 4.50. *Astron. Astrophys.* **364**, L54.

BOYNTON W. V., EVANS L. G., REEDY R. C. AND TROMBKA J. I. (1993) Determination of planetary composition by in-situ and remote gamma-ray spectrometry. In *Remote Geochemical Analysis: Elemental and Mineralogical Composition* (eds. C. Pieters and P. Englert), pp. 395–411. Cambridge University Press, New York, New York, USA.

BOYNTON W. V. *ET AL.* (2000) Scientific objectives of the *Mars Surveyor 2001* gamma-ray spectrometer (abstract). In *Second International Conference on Mars Polar Science and Exploration, August 21-25, 2000, Reykjavik, Iceland* (eds. G. Ryder and V. L. Sharpton). Lunar and Planetary Institute, Contribution No. **1057**, #4106, Houston, Texas, USA.

CLARK P. E., TROMBKA J. AND FLOYD S. (1995) Solar monitor design for the NEAR x-ray spectrometer (abstract). *Lunar Planet. Sci.* **26**, 253–254.

EVANS L. G., REEDY R. C. AND TROMBKA J. I. (1993) Introduction to planetary remote-sensing. In *Remote Geochemical Analysis: Elemental and Mineralogical Composition* (eds. C. Pieters and P. Englert), pp. 167–198. Cambridge University Press, New York, New York, USA.

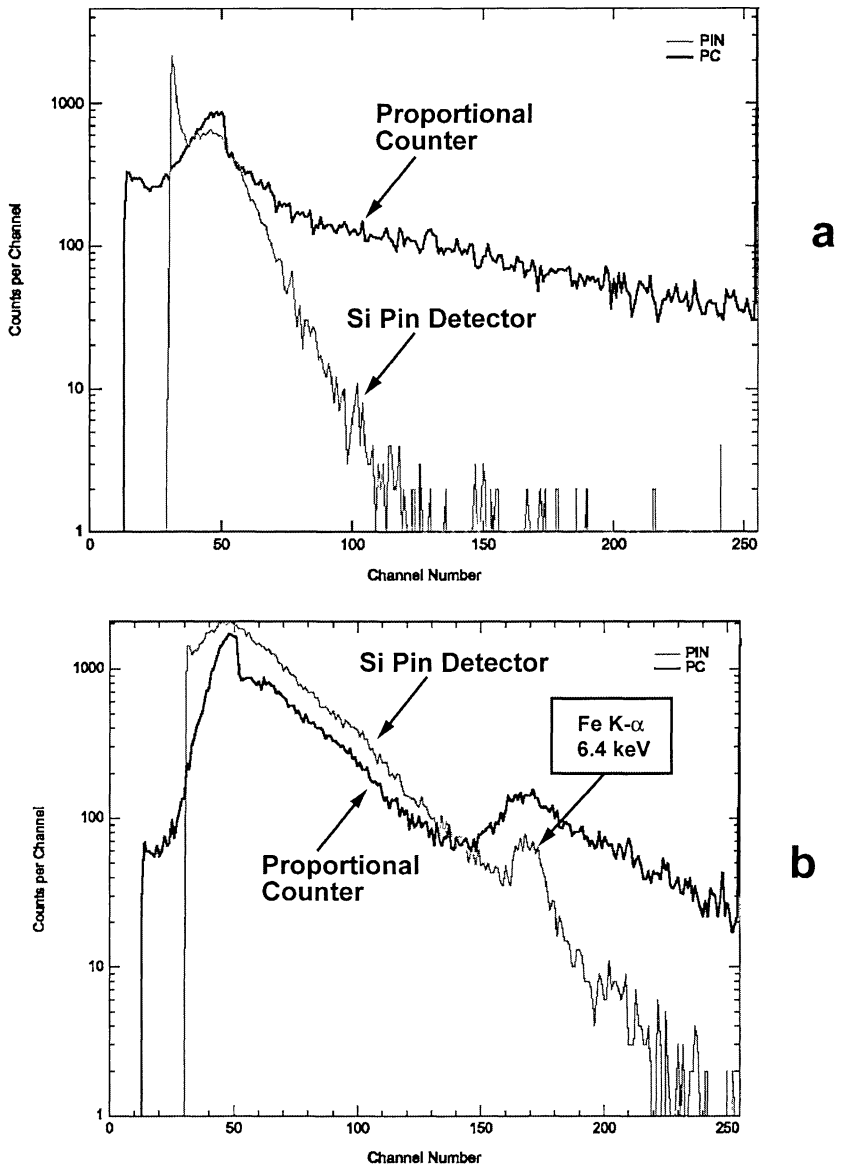

FIG. 6. Proportional counter and PIN detector pulse height spectra measured during (a) a quiet Sun period and (b) a solar flare period.

EVANS L. G., STARR R., TROMBKA J. I., MCCLANAHAN T. P., BAILEY S. H., MIKHEEVA I., BHANGOO J., BRÜCKNER J. AND GOLDSTEN J. O. (2000) Calibration of the NEAR gamma-ray spectrometer. *Icarus* **148**, 95–117.

EVANS L. G., TROMBKA J. I., STARR R. D., BOYNTON W. V., BRÜCKNER J. AND REEDY R. C. (2001a) Preliminary results of the NEAR gamma-ray spectrometer (abstract). *Lunar Planet. Sci.* **32**, #1812, Lunar and Planetary Institute, Houston, Texas, USA (CD-ROM).

EVANS L. G., STARR R. D., BRÜCKNER J., REEDY R. C., BOYNTON W. V., TROMBKA J. I., GOLDSTEN J. O., MASARIK J., NITTLER L. R. AND MCCOY T. J. (2001b) Elemental composition from gamma-ray spectroscopy of the NEAR–Shoemaker landing site on 433 Eros. *Meteorit. Planet. Sci.* **36**, 1639–1660.

FELDMAN W. C., BINDER A. B., HUBBARD G. S., MCMURRAY R. E., JR., MILLER M. C. AND PRETTYMAN T. P. (1996) The Lunar Prospector gamma-ray spectrometer (abstract). *Lunar Planet. Sci.* **27**, 355–356.

FICHTEL C. E. AND TROMBKA J. I. (1997) *Gamma-ray Astrophysics, New Insight into the Universe.* NASA Special Publication **1386**, Greenbelt, Maryland, USA. 376 pp.

GOLDSTEN J. O. *ET AL.* (1997) The x-ray/gamma-ray spectrometer on the near-Earth asteroid rendezvous mission (abstract). *Space Sci. Rev.* **82**, 169.

HASEBE N. *ET AL.* (1999) Gamma-ray spectrometer for Japanese lunar polar orbiter. *Adv. Space Res.* **23**, 1837–1840.

HURLEY K. *ET AL.* (2000) Interplanetary network localization of GRB 991208 and the discovery of its afterglow (abstract). *Astrophys. J. Lett.* **534**, 23.

JENSEN B. L. *ET AL.* (2001) The afterglow of the short/intermediate-duration gamma-ray burst GRB 000301c: A jet at Z = 2.04. *Astron. Astrophys.* **370**, 909–922.

JOLLIFF B. L., GILLIS J. J., HASKIN L. A., KOROTEV R. L. AND WIECZOREK M. A. (2000) Major lunar crustal terranes: Surface expressions and crust-mantle origins. *J. Geophys. Res.* **105**, 4197–4416.

KLOSE S. *ET AL.* (2000) The very red afterglow of GRG 000418: Further evidence for dust extinction in a gamma-ray burst host galaxy. *Astrophys. J.* **545**, 271–276.

KURCZYNSKI P. *ET AL.* (1999) Long-term radiation damage to a spaceborne germanium spectrometer. *Nuc. Instrum. Methods Phys. Res.* **A431**, 141–147.

LAWRENCE D. J., FELDMAN W. C., BARRACLOUGH B. L., BINDER A. B., ELPHIC R. C., MAURICE S. AND THOMSEN D. R. (1998) Global element maps of the Moon: The Lunar Prospector gamma-ray spectrometer. *Science* **281**, 1484–1489.

LEDERER C. M. AND SHIRLEY V. S. (EDS.) (1978) *Table of Isotopes Eighth Edition.* Wiley, New York, New York, USA. 1628 pp.

MCCOY T. J. *ET AL.* (2001) The composition of 433 Eros: A mineralogical–chemical synthesis. *Meteorit. Planet. Sci* **36**, 1661–1672.

NITTLER L. R. *ET AL.* (2001) X-ray fluorescence measurements of the surface elemental composition of asteroid 433 Eros. *Meteorit. Planet. Sci.* **36**, 1673–1695.

OWENS A. *ET AL.* (1995) A high resolution spectrometer for gamma-ray burst astronomy. *Space Sci. Rev.* **71**, 273–296.

STARR R. S., CLARK P. E., EVANS L. G., FLOYD S. R., MCCLANAHAN T. P., TROMBKA J. I., GOLDSTEN J. O., MAURER H., MCNUTT R. L., JR. AND ROTH D. R. (1999a) Radiation effects in the Si-PIN detector on the near-Earth asteroid rendezvous Mission. *Nucl. Instrum. Methods Phys. Res.* **A428**, 209.

STARR R. *ET AL.* (2000) Instrument calibration and data analysis procedures for the NEAR x-ray spectrometer. *Icarus* **147**, 498–519.

TROMBKA J. I. *ET AL.* (1997) Compositional mapping with the NEAR x-ray/gamma-ray spectrometer. *J. Geophys. Res.* **102**, 23 729–23 750.

TROMBKA J. I. *ET AL.* (2000a) The elemental composition of asteroid 433 Eros: Results of the NEAR–Shoemaker x-ray spectrometer. *Science* **289**, 2101–2105.

TROMBKA J. I. *ET AL.* (2000b) The chemical composition of asteroid 433 Eros: Preliminary results of the NEAR-Shoemaker x-ray/gamma-ray spectrometer (abstract). *Meteorit. Planet. Sci.* **35 (Suppl.)**, A160.

VEVERKA J. *ET AL.* (1997) NEAR's flyby of 253 Mathilde: Images of a C asteroid. *Science* **278**, 2109.

YIN L. I., TROMBKA J. I., ADLER I. AND BIELEFELD M. (1993) X-ray remote-sensing techniques for geochemical analysis of planetary surfaces. In *Remote Geochemical Analysis: Elemental and Mineralogical Composition* (eds. C. Pieters and P. Englert), pp. 199–212. Cambridge University Press, New York, New York, USA.